

Effects of Unsymmetrical Voltage Sags on Industrial Adjustable Speed Drives*

Milutin P. Petronijević^{1,a}, Nebojša N. Mitrović¹,
Vojkan Z. Kostić¹, Bojan G. Banković¹

Abstract: This paper researches unsymmetrical voltage sag influence on torque ripple in scalar controlled (V/Hz), rotor field oriented (RFO) and direct torque controlled (DTC) drives. Electric drives performance degradation during voltage sag mainly depends on the used control algorithm. Industrial drives with all three types control methods are experimentally tested. Experiments with digital observer's application confirm the proposed solution.

Keywords: Adjustable speed drives, Power quality, Voltage sag, Torque ripple, Disturbance observer.

1 Introduction

Sensitivity of adjustable speed drives (ASDs) to voltage sags was a subject of numerous studies and experimental researches [1-5]. The main criteria for determining the threshold sensitivity is the input voltage value that causes the disconnection/tripping of frequency converter. From previous researches, it is known fact that the voltage sags, especially unsymmetrical, can cause ASDs performance degradation, primarily reduction of available motor torque [2] and the occurrence of significant dc link voltage ripple [3]. The unsymmetrical voltage sag influence on AC drives is analyzed in [4], while in the literature [5] was also presented some experimental results and under-voltage protection limit settings related to different unsymmetrical voltage sag types in order to overcome the device tripping.


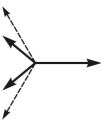
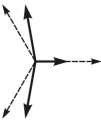
Previously led analytical and experimental researches in the sensitivity analysis did not take into account the type and ac drives control performance. This paper experimentally verifies interaction applied control method with the unsymmetrical voltage sags, especially in high-performance drives. Single-line-to-ground faults (SLGFs), which are the most frequent types of fault system (responsible for around 70% of all faults, [6]), have resulted in voltage sag types

¹Power Department, Faculty of Electronic Engineering, University of Niš, Aleksandra Medvedeva 14, 18000 Niš, Serbia; E-mail: ^amilutin.petronijevic@elfak.ni.ac.rs

*Award for the best paper presented in Section *Power Engineering*, at Conference ETRAN 2009, June 15-19, Vrnjačka Banja, Serbia.

B, C and D. Phase voltage equations in complex form and the appropriate phasor diagrams that illustrate the above basic unsymmetrical sag types were given in **Table 1**. Frequency converter of the some manufacturer will not lead to failure, but it will certainly lead to performance deterioration. Number of these types of faults and the fact that the dc link voltage remains above the under-voltage protection limit, have encouraged consideration of possibilities for the elimination of unwanted torque ripple, while maintaining the quality of speed/torque regulation.

Table 1
Basic types of unsymmetrical voltage sags.

Sag type	Phasor diagram (solid lines during fault)	Phase-to-neutral voltages (<i>h</i> designates remain voltage in p.u.)
B		$U_a = \frac{1}{2}U; \quad U_b = -\frac{1}{2}U - j\frac{\sqrt{3}}{2}U;$ $U_c = -\frac{1}{2}U + j\frac{\sqrt{3}}{2}U$ <p>Remain voltage range: $h=0...1$</p>
C		$U_a = U; \quad U_b = -\frac{1}{2}U - j\frac{\sqrt{3}}{2}hU;$ $U_c = -\frac{1}{2}U + j\frac{\sqrt{3}}{2}hU$ <p>Remain voltage range: $h=0.333...1$</p>
D		$U_a = hU; \quad U_b = -\frac{1}{2}hU - j\frac{\sqrt{3}}{2}U;$ $U_c = -\frac{1}{2}hU + j\frac{\sqrt{3}}{2}U$ <p>Remain voltage range: $h=0.333...1$</p>

The paper first analyzes the correctness of the analytical relations regarding to the electromagnetic torque ripple. The obtained analytical results are valid only for scalar (V/Hz) control, while in the case of drives with the rotor field oriented (RFO) and direct torque control (DTC) algorithms is apparent motor torque ripple effect reduction. Some extent sensitivity of RFO controlled drives

on dc voltage ripple impact initiate in this paper to be proposed modification of the inner, current control loop by adding the disturbance observer. It was found that the classical DTC drives are nearly insensitive to this type of power quality disturbance, indeed with less sensitivity in the case of application of modified control methods with a constant switching frequency and PI controllers for flux and electromagnetic motor torque. Experimental tests on the modified industrial converter confirm the derived conclusions and demonstrate the effectiveness of the applied methods for the disturbance elimination.

2 Adjustable Speed Drives

Numerous industrial applications set the requirements for dynamic performance in the background, especially where no sudden changes in speed or torque loads or multi-motor drives supplied from a common frequency converter are concerned. Variable speed drives in these cases are implemented with a scalar control with or without speed feedback. The basic, constant V/Hz control can be modified to offset the voltage drop across the inverter and stator resistance, which usually has a significant impact at low output frequencies/speeds. The simplest, well-known control structure is shown in Fig. 1 where the stator terminal voltage shaping implemented using space vector pulse width modulation (SV-PWM) technique.

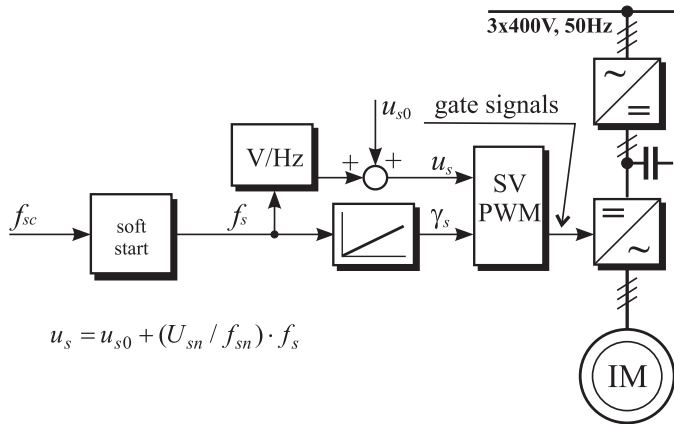


Fig. 1 – Basic V/Hz control scheme.

As industrial standards for ASDs with high and medium dynamic performance, requirements now imposed the two main solutions, which allow electromagnetic torque control:

- **Vector control:** based on stator current control in synchronous reference system using inverter switching transistor pulse width modulation.

- **Direct torque control (DTC):** based on stator flux phasor position control, basically, with two hysteresis controllers, one for the stator flux amplitude and the other one for electromagnetic torque instantaneous value.

Illustration of the basic control structure that uses indirect rotor flux oriented control (designated by RFO in this paper) is shown in Fig. 2. It can be seen two basic control contours for d - and q -stator current components. Typically, it is used two linear, proportional-integral (PI) controllers. Basic equations for proportional (K_p) and integral (K_i) gain adjusting for q - and d -current loops, considering decoupling circuit influence, are shown in [7]. In the experiments conducted in the paper, current control loop bandwidth is set to 1250rad/s, which is practically the limit, imposed by the presence of the noise in the measured currents. Digital PI controllers in d - and q -axis are identical and have parameters $K_p = 21.75$ and $K_i = 0.768$ where the sampling period of fast current control contours set at 100 μ s.

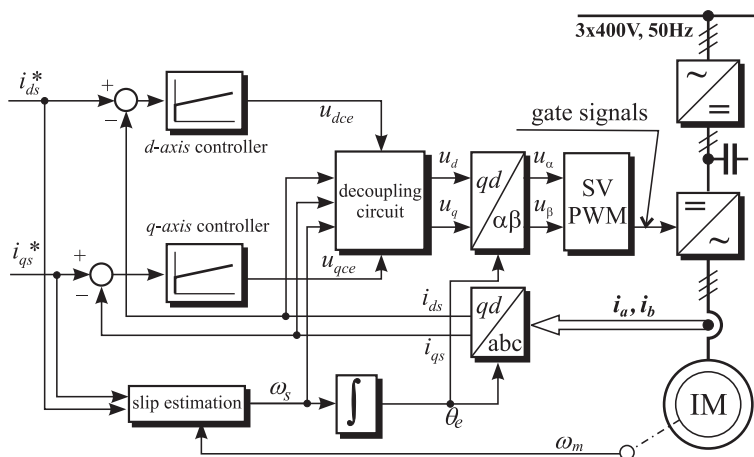


Fig. 2 – Basic RFO control scheme.

Direct torque control in the basic variant has hysteresis controllers for flux and electromagnetic torque. To achieve acceptable torque ripple it is needed to determine switching transistor state in time, which is about ten times shorter ($\approx 25\mu$ s) than switching frequency. Using identical hardware platform required the implementation of the modified DTC method with linear torque and flux PI controllers with sampling time as the RFO method. The basic structure of the modified DTC method is shown in Fig. 3. Constant switching frequency is achieved by using space vector pulse-width modulation method (SV-PWM). Parameters adjusting of PI controllers were initially derived from the

recommendations given in [9] using symmetric optimum method. During the experiment parameters were additionally adjusted to achieve torque control loop bandwidth equal to 1250 rad/s, which is the same with RFO current control loops bandwidths. Digital PI controllers have parameters: for torque $K_{pT} = 16.875$ and $K_{iT} = 0.125$, and for flux $K_{p\psi} = 2499.875$ and $K_{i\psi} = 0.125$.

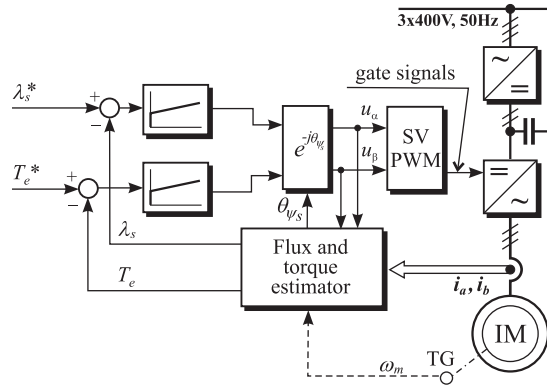


Fig. 3 – Modified DTC control scheme.

Unsymmetrical voltage sag impact researches was conducted in torque control mode (outer speed control loop is put aside) to eliminate the effect of speed controller on torque ripple.

3 Unsymmetrical Voltage Sag Effects

In case of B, C or D voltage sag, input rectifier passes into single-phase operations with the consequences as input current distortion and DC voltage ripple increase with dominant component at 100Hz and with average voltage reduction in C type voltage sag case. DC bus voltage $v_{dc}(t)$ in case of a voltage sag supply conditions, regarding [3] it can be presented as:

$$v_{dc}(t) = V_{DC} + V_{DC2} \cos(2\omega_i t + \theta_2) \quad (1)$$

where V_{DC} presents an average voltage value, V_{DC2} is the second voltage harmonic, ω_i is power supply angular frequency ($2\pi 50s^{-1}$ or $2\pi 60s^{-1}$) and θ_2 is an appropriate angle of the second harmonic component referring to d -axis which defines point on wave at sag initiation.

Output inverter part of frequency converter by suitable pulse width modulation control turns dc voltage into induction motor stator terminal ac voltage. Generally, modulation signal can be presented as ([10]):

$$u_i(t) = u_i^*(t) + e_i(t) \quad (2)$$

where $e(t)$ is injected harmonic (also represents direct transformation SVPWM into carrier based PWM), and $u_i^*(t)$ are called fundamental signals for appropriate phase voltages ($i = a, b, c$). Fundamental components of line to neutral output PWM voltages are:

$$\begin{aligned} u_{an}(t) &= \frac{1}{2} v_{dc}(t) [m \sin(\omega_{out} t + \varphi) + e_i(t)], \\ u_{bn}(t) &= \frac{1}{2} v_{dc}(t) \left[m \sin\left(\omega_{out} t - \frac{2\pi}{3} + \varphi\right) + e_i(t) \right], \\ u_{cn}(t) &= \frac{1}{2} v_{dc}(t) \left[m \sin\left(\omega_{out} t + \frac{2\pi}{3} + \varphi\right) + e_i(t) \right], \end{aligned} \quad (3)$$

where ω_{out} - inverter output fundamental frequency with modulation index m . Phase angle φ corresponds to initial phase voltage angle related to d axis.

Combining equations (2) and (3), and applying coordinate transformations, induction motor stator voltages in dq reference frame that rotates at a synchronous reference speed ω_{out} , are:

$$\begin{aligned} u_{ds}(t) &= \frac{1}{2} m [V_{DC} \cos \varphi + V_{DC2} \cos(2\omega_t t + \theta_2) \cos \varphi], \\ u_{qs}(t) &= \frac{1}{2} m [V_{DC} \sin \varphi + V_{DC2} \cos(2\omega_t t + \theta_2) \sin \varphi]. \end{aligned} \quad (4)$$

In equations above the second term is a direct consequence of dc link voltage ripple because of rectifier single-phase operation. Based on equation (4) we also conclude that the modulation type varying (different injected harmonics) has no influence on additional, undesired d - and q - axis voltage components.

According to [3] voltage sag type, dc bus circuit parameters and load value influence on stator voltage ripple. Taking into account that inverter and motor overall behave as a dynamic load, it very difficult analytically calculate second harmonic voltage V_{DC2} value accurately, and with itself predict unwanted torque ripple. Besides, previous relations do not take into account fast current/torque control loops effects existing in high performance drives.

Combining the equations (4) with dq synchronous reference frame induction motor equations can be calculated instantaneous torque value in the closed form:

$$T_e = T_{e0} + T_{e2} \cos(2\omega_t t + \varphi_2) + T_{e4} \cos(4\omega_t t + \varphi_4), \quad (5)$$

where T_{e0} represents average torque value, T_{e2} represents the second harmonic component and T_{e4} represents the fourth harmonic components. Details about formula derivation can be found in [3], but the achieved results can be cautiously accepted as valid, only for drives with V/Hz control. Motor torque oscillatory component presence can, beside noise increase, leads to mechanical resonance exciting in coupled multi-motor drives for example in paper production machines.

In high performance drives, especially in DTC drives, we expect that unwanted torque pulsation will be remarkably restrained if the inner control loops bandwidth is wider than the dominant second harmonic frequency (100Hz). Stator current components or torque control loops adjusting satisfy this requirement.

4 Results

The ASD prototype with different control algorithms is implemented by using DSP system based on dSpace DS1104 control board, Matlab/Simulink software with RTI toolbox and with ControlDesk software for experiment performing and capturing results. The experimental verification of the theoretical results was carried out at drive system which consists of the modified Danfoss VLT5000 series industrial frequency converter which nominal power is 3.1 kVA, an TTL pulse encoder (1024 pulse/revolution) was mounted on induction motor (rated power 2.2 kW) at drive shaft end.

Mechanical load of the induction motor was done by AC servo drive, which was directly coupled with motor under test. Simple unsymmetrical voltage sag generator was constructed using three-phase power transformer rated power 15 kVA with the tap changer under load and with one autotransformer on transformer primary side. Induction motor and adjustable speed drives data are given in **Table 2**.

Table 2
Motor data (per phase) and ASD parameters.

Rated power /speed	2200W/2835rpm
Stator voltage U_s	230V
Stator resistance R_s	2.7 Ω
Stator leakage inductance L_{ls}	10.5mH
Rotor resistance R_r	2.2 Ω
Rotor leakage resistance L_{lr}	10.5mH
Mutual inductance M	270mH
Motor inertia J_m	0.00184kgm ²
Total leakage coefficient σ	0.073
DC link capacitance (C_f)	2 \times 330 μ F(in series)
DC link inductance (L_f)	2 \times 3.6mH

RFO controlled drive’s current control subsystem, coordinate transformation blocks, decoupling circuit and slip calculation estimator were realized digitally with the sample time equal to 100 μ s. Slower speed control loop was implemented with 10 ms sample time. Switching frequency of symmetrical SV-PWM modulation is set at 5 kHz, which also presents simultaneous sampling frequency for two stator currents. In DTC drive torque and flux control loops calculation time-period set to 100 μ s. Sampling time regarding to speed control loop and SVPWM switching frequency are equal to RFO drive settings.

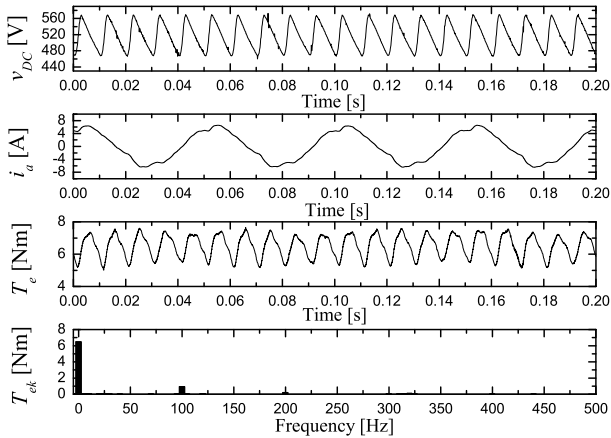


Fig. 4 – *B type voltage sag effect in drive with V/Hz control method (load torque = 80% rated, output frequency = 20Hz).*

Illustration of conclusion from (5) was given in Fig. 4 where single-phase B type voltage sag consequences were taken out. Dominant second harmonics in dc voltage and consequently in estimated motor torque are clearly noticeable. Induction motor stator currents distortion can also be seen.

Vector controlled drive was firstly nominally loaded in torque control mode. At the time close to $t = 0.24$ s at frequency converter terminal one phase input voltage reduced to zero level which responded to voltage sag B type.

In Fig. 5 estimated motor torque waveform was presented which is evident the presences of unwanted torque oscillations significantly reduced, but also exist at the same characteristic frequencies as in V/Hz drives.

One of the simplest methods for this periodic pulsation reduction is Q -disturbance observer application [11] in current control loop, which, in our case, is incorporated only in q -axis. In Fig. 6 it was shown, in continuous time domain, realized disturbance observer along with stator transfer function $G_s(s)$ and with transfer function $G_{mv}(s)$ which takes into account inverter voltage

gain and delay. Transfer function designated as $G_n(s)$ is a nominal, open loop transfer function calculated as a series connection of $G_s(s)$ and $G_{inv}(s)$ for nominal motor parameters given in **Table 1**. Disturbance observer subsystem was also digitally realized with sample time equal to 100 μ s.

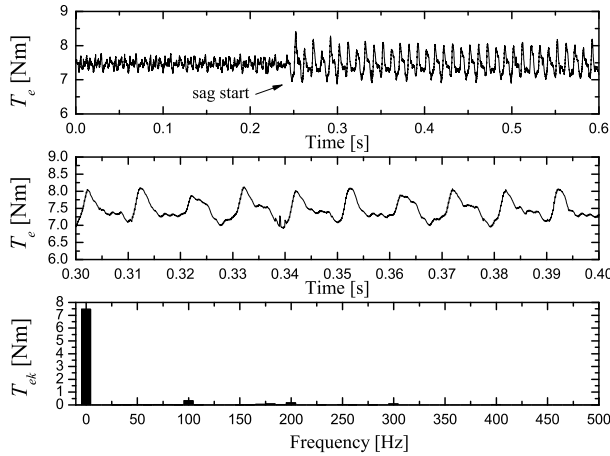


Fig. 5 – *B* type voltage sag effect on RFO controlled ASD (load torque = 100% rated).

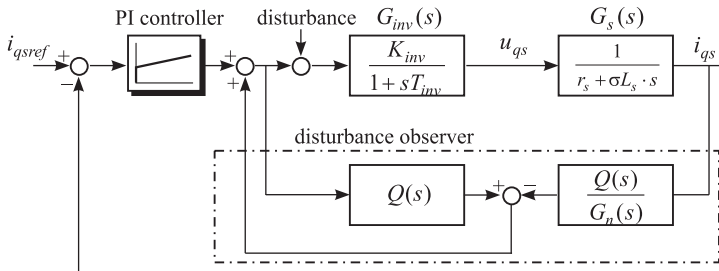


Fig. 6 – *Disturbance observer incorporation into q-axis control loop* ($Q(s) = 0.5(1 + 0.0008s)^{-2}$).

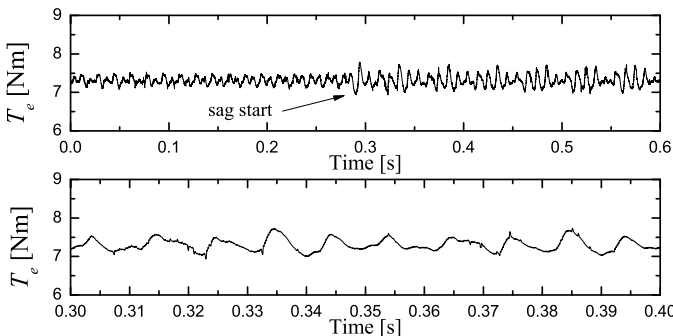


Fig. 7 – *B* type voltage sag effect in drive with RFO control (load torque = 100% rated, Q observer application)

In Fig. 7 unwanted torque oscillation decrease after sag initiation is observed. Ripple reduction is almost two times comparing to regime without disturbance observer application. In the experiment limitation posed by measured currents noise existing suppress Q -observer effectiveness. Besides, it should be mentioned that the torque oscillations would significantly increase at higher output frequencies at same load torque. Named facts give us guidelines to design advanced disturbance observers due to efficient ripple reduction.

DTC motor drive was also tested on B type sag influence initiated at $t = 0.2\text{s}$. In Fig. 8 can be seen DTC drive practically with low voltage sag induced torque ripple sensitivity.

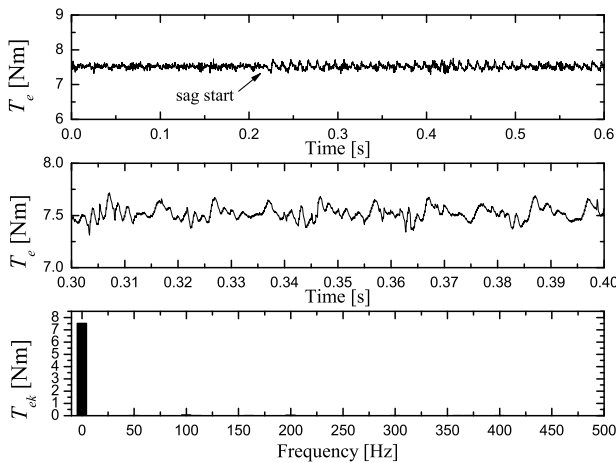


Fig. 8 – B type voltage sag effect in drive with DTC control (load torque = 100% rated).

5 Conclusion

High performance ASDs with RFO and DTC control, during voltage sag, have complex response regarding to motor speed reduction and electromagnetic torque oscillation appearing. Simplified analysis, which does not respect control algorithm effects, shows no accurate results regarding to drive behaviour during the voltage sags.

Based on numerous simulation and experimental results it was identified the significant differences in ASD behaviour during unsymmetrical voltage sag events. Fast current/torque control loops have most important influence on torque oscillatory components value. Disturbance observer application at RFO controlled drives can considerably reduce unwanted torque ripple. Further researches will be directed to advanced disturbance estimator application but it will be with great importance in drives with low dc link capacitance values.

6 References

- [1] S.Z. Djokic, K. Stockman, J.V. Milanovic, J.J.M. Desmet, R. Belmans: Sensitivity of AC Adjustable Speed Drives to Voltage Sags and Short Interruptions, *IEEE Transaction on Power Delivery*, Vol. 20, No. 1, Jan. 2005, pp. 494 – 505.
- [2] M.P. Petronijevic, B.I. Jeftenic, N.M. Mitrovic, V.Z. Kostic: Voltage Sag Drop in Speed Minimization in Modern Adjustable Speed Drives, *IEEE International Symposium on Industrial Electronics*, June 2005, Vol. 3, pp. 929 – 934.
- [3] K. Lee, T.M. Jahns, W.E. Berkopec, T.A. Lipo: Closed-form Analysis of Adjustable Speed Drive Performance under Input Voltage Unbalance and Sag Conditions, *IEEE Transaction on Industrial Application*, Vol. 42, No. 3, May/June 2006, pp. 733 – 741.
- [4] M.H.J. Bollen, L.D. Zhang: Analysis of Voltage Tolerance of AC Adjustable-speed Drives for Three-phase Balanced and Unbalanced Sags, *IEEE Transaction on Industrial Application*, Vol. 36, No. 3, May/June 2000, pp. 904 – 910.
- [5] K. Stockman, F. D'hulster, K. Verhaege, M. Didden, R. Belmans: Ride-through of Adjustable Speed Drives During Voltage Dips, *Electric Power System Research*, Vol. 66, No. 1, July 2003, pp. 49 – 58.
- [6] M.H.J. Bollen, *Understanding Power Quality Problems: Voltage Sags and Interruptions*, IEEE Press Marketing, New York, 2000.
- [7] D. Telford, M.W. Dunnigan, B.W. Williams: Online Identification of Induction Machine Electrical Parameters for Vector Control Loop Tuning, *IEEE Transaction on Industrial Electronics*, Vol. 50, No. 2, April 2003, pp. 253 – 261.
- [8] Y.S. Lai, J.H. Chen: A New Approach to Direct Torque Control of Induction Motor Drives for Constant Inverter Switching Frequency and Torque Ripple Reduction, *IEEE Transaction On Energy Conversion*, Vol. 16, No. 3, Sept. 2001, pp. 220 – 227.
- [9] M.P. Kazmierkowski, R. Krishnan, F. Blaabjerg: *Control in Power Electronics – Selected problems*, Academic Press, New York, 2002.
- [10] K. Zhou, D. Wang: Relationship between Space-vector Modulation and Three-phase Carrier-based PWM: A Comprehensive Analysis [Three-phase Inverters], *IEEE Transaction on Industrial Electronics*, Vol. 49, No. 1, Feb. 2002, pp. 186 – 196.
- [11] Y. Choi, K. Yang, W.K. Chung, H.R. Kim, I.H. Suh: On the Robustness and Performance of Disturbance Observer for Second-order Systems, *IEEE Transaction on Automatic Control*, Vol. 48, No. 2, Feb. 2003, pp. 315 – 320.